Photodissociation Cross Section of ClOOCl at 330 nm

ARTICLE *in* THE JOURNAL OF PHYSICAL CHEMISTRY A · APRIL 2010

Impact Factor: 2.69 · DOI: 10.1021/jp909374k · Source: PubMed

Photodissociation Cross Section of ClOOCl at 330 nm†

Bing Jin,[‡,§] I-Cheng Chen,[‡] Wen-Tsung Huang,[‡,||] Chien-Yu Lien,[‡] Nikhil Guchhait,[‡,⊥] and Jim J. Lin*[,‡,||]

Institute of Atomic and Molecular Sciences, Academia Sinica, Taipei 10617, Taiwan, State Key Laboratory of Molecular Reaction Dynamics, Dalian Institute of Chemical Physics, Chinese Academy of Science, Dalian, 116023, China, Department of Chemistry, National Taiwan University, Taipei 10617, Taiwan, and Department of Chemistry, University of Calcutta, Kolkata 700009, India

Received: September 29, 2009; Revised Manuscript Received: December 15, 2009

The photolysis rate of ClOOCl is crucial in the catalytic destruction of polar stratospheric ozone. In this work, we determined the photodissociation cross section of ClOOCl at 330 nm with a molecular beam and with mass-resolved detection. The photodissociation cross section is the product of the absorption cross section and the dissociation quantum yield. We formed an effusive molecular beam of ClOOCl at a nozzle temperature of 200 or 250 K and determined its photodissociation probability by measuring the decrease of the ClOOCl intensity upon laser irradiation. By comparing with a reference molecule (Cl_2), of which the absorption cross section and dissociation quantum yield are well-known, we determined the absolute photodissociation cross section of ClOOCl at 330 nm to be $(2.31 \pm 0.11) \times 10^{-19}$ cm^2 at 200 K and $(2.47 \pm 0.12) \times 10^{-19}$ cm^2 at 250 K. Impurity interference has been a well-recognized problem in conventional spectroscopic studies of ClOOCl; our mass-resolved measurement directly overcomes such a problem. This measurement of the ClOOCl photolysis cross section at 330 nm is particularly useful in constraining its atmospheric photolysis rate, which in the polar stratosphere peaks near this wavelength.

Introduction

ClOOCl plays a central role in catalytic chemical processes in the ozone hole formation.[1−7] The following chemical reactions indicate a catalytic cycle: the photolysis of ClOOCl generates Cl atoms (R1a); Cl atoms quickly react with O_3 to form ClO radicals (R2); two ClO radicals can then dimerize to form ClOOCl again (R3), thus destroying O_3 catalytically.

$$\mathrm{ClOOCl} + h\nu \rightarrow 2\,\mathrm{Cl} + \mathrm{O_2} \qquad \text{(R1a)}$$

$$(\mathrm{Cl} + \mathrm{O_3} \rightarrow \mathrm{ClO} + \mathrm{O_2}) \times 2 \qquad \text{(R2)}$$

$$\mathrm{ClO} + \mathrm{ClO} + \mathrm{M} \rightleftarrows \mathrm{ClOOCl} + \mathrm{M} \qquad \text{(R3)}$$

$$\text{Net: } 2\mathrm{O_3} + h\nu \rightarrow 3\mathrm{O_2} \qquad \text{(R4)}$$

The photolysis of ClOOCl (R1a) is the rate-determining step which controls the overall efficiency of the catalytic cycle. The quantum yield of R1a is believed to be close to unity (discussed below). If the photolysis of ClOOCl produced ClO, O_3 would not be destroyed because the overall process becomes a null cycle:

$$\mathrm{ClOOCl} + h\nu \rightarrow 2\,\mathrm{ClO} \qquad \text{(R1b)}$$

$$\mathrm{ClO} + \mathrm{ClO} + \mathrm{M} \rightleftarrows \mathrm{ClOOCl} + \mathrm{M} \qquad \text{(R3)}$$

Large discrepancy in laboratory data of the absorption cross sections of ClOOCl causes large uncertainty in estimating the rate of R1a, which is the product of the absorption cross section, the solar irradiation, and the Cl quantum yield. Notably, Pope et al.[8] reported in 2007 spectroscopic measurements of ClOOCl with new methods of sample preparation, which resulted in spectra with low impurity levels and high peak absorbances. However, these newly reported absorption cross sections[8] in the critical wavelength region of 300−400 nm are much smaller than the 2006 Jet Propulsion Laboratory (JPL) recommended values[9] and other previous measurements of ClOOCl absorption cross sections.[10−14] The atmospheric photolysis rate resulting from Pope et al. cross sections[8] would therefore be much slower than previously thought and could not explain the observed polar stratospheric ozone loss in current photochemical models. If the result of Pope et al. was correct, it would imply there is a substantial deficiency in the current ozone depletion models.[3,5,15] Several recent studies[16−19] have cast doubt on the Pope et al. data,[8] but there are still significant discrepancies, and high precision measurements allowing an accurate determination of atmospheric photolysis rates are highly desirable.

Although there have been many measurements on the absorption spectrum of ClOOCl,[2,7,8,10−14] difficulties in subtracting the impurity contributions may cause larger error bars of the ClOOCl cross sections, especially in the long wavelength tail where the ClOOCl absorbs rather weakly and the absorbance from impurities is much higher. Recently, we reported a method that utilizes mass-selected detection to directly overcome the impurity problems.[17] We formed an effusive ClOOCl molecular beam and measured the number density of ClOOCl before and

‡ Institute of Atomic and Molecular Sciences.
§ Chinese Academy of Science.
|| National Taiwan University.
⊥ University of Calcutta.
† Part of the special section "30th Free Radical Symposium".
* To whom correspondence should be addressed. E-mail: jimlin@gate.sinica.edu.tw.

10.1021/jp909374k
Published on Web 01/19/2010

after the laser irradiation with a mass detector. The ClOOCl molecules in the molecular beam were depleted due to photodissociation; the probability of photodissociation is proportional to the laser fluence I, absorption cross section σ, and dissociation quantum yield ϕ. We then determined the absolute photodissociation cross sections $\sigma\phi$ of ClOOCl at two excimer wavelengths (XeCl 308 nm and XeF 351 nm) by comparing its depletion signal with that of a reference molecule of which the absorption cross section and dissociation quantum yield have been well measured. Our results strongly suggest that the UV absorption cross sections of ClOOCl are consistent with the current O_3 depletion models. Furthermore, we also measured the ClOOCl cross sections at 248 and 266 nm with the same method. The results[20] indicate that the absorption cross section of ClOOCl was significantly underestimated even at the peak wavelength (~245 nm) of the spectrum. If we renormalize a few relative measurements[8,12,16] of ClOOCl cross sections to our new cross section at 248 nm, the overall consistency at other wavelengths (≤308 nm) would be greatly improved.[20]

Because light at wavelengths shorter than 300 nm is strongly absorbed by ozone, irradiation at longer wavelengths is most significant for ClOOCl photolysis in the atmosphere. Although our previous data at 308 and 351 nm[17] have set constraints for the atmospheric photolysis rates of ClOOCl, to better estimate these rates more measurements of high accuracy at other wavelengths would be very helpful.

In this study, we utilized a multipass technique of the laser beam to increase the effective laser fluence, such that a dye laser could produce a similar signal-to-noise ratio in comparison to the previously used excimer or Nd:YAG laser which was much more intense. Here we report the absolute photodissociation cross section of ClOOCl at 330 nm at two temperatures, 200 and 250 K. From the reported absorption spectra of ClOOCl,[9−19] the wavelength-resolved photolysis rate of ClOOCl would peak near 330 nm under typical atmospheric conditions of the ozone hole formation.[8,15,19] In addition, because the absorption spectrum of Cl_2 also peaks near 330 nm, subtraction of the inevitable Cl_2 impurity becomes more sensitive at this wavelength in determining the ClOOCl cross section in conventional measurements. Therefore, this work provides a very important checkpoint in estimating the atmospheric photolysis rate of ClOOCl.

Experimental Section

The experimental apparatus has been described elsewhere;[17,20,21] only the relevant setup is given here. The ClOOCl sample was synthesized following the Method 1 reported by Pope et al. ($Cl_2 + h\nu \rightarrow 2Cl$; $Cl + O_3 \rightarrow ClO + O_2$; $2ClO + M \rightarrow ClOOCl + M$).[8] We made two modifications for our convenience: (i) the photolysis wavelength to dissociate Cl_2 was 355 nm (Nd:YAG laser, 80 mJ/pulse, 10 Hz, 8 mm diameter) instead of 351 nm (XeF excimer laser); (ii) O_2 (99.997%, Air Products and Chemicals, Inc., 1.1 bar) was used as the buffer gas.

The ClOOCl was synthesized in a flow tube made of fused silica at about 200 K and trapped in another fused silica tube at a low temperature around 150 K. After synthesis and trapping for about 40 min, the gas mixture was pumped out and the ClOOCl molecules were left in a solid form. Upon slowly warming up the trap (154−158 K in 3 h), the solid ClOOCl evaporated, and then an effusive molecular beam of ClOOCl was formed by allowing the low-pressure sample to flow through a capillary array (5 square holes of 0.5 mm × 0.5 mm, horizontally aligned) made of fused silica. The sample pressure behind the nozzle was controlled by the trap temperature to be less than 0.1 mbar to ensure an effusive flow, in which the gas mean free path exceeds the nozzle dimensions and the velocity distribution does not depend on the pressure. In such an effusive molecular beam, the molecules are in thermal equilibrium with the nozzle wall; the temperature reported here is referred to as the nozzle temperature. The velocity distribution of the effusive molecular beam basically followed a Maxwell−Boltzmann distribution. Analysis on the arrival time profiles indicated a small amount of translational cooling of 10−20 K. Since vibrational cooling is much less efficient than the translational cooling, the vibrational temperature of the effusive beam would be very close to the nozzle temperature.

The molecular beam was then chopped, collimated,[17] irradiated by a laser beam, and eventually monitored with a time-resolved quadrupole mass spectrometer.[21] In the photolysis volume, the sample pressure was less than 10^{-6} mbar. In a typical experimental run, the evaporated ClOOCl sample could last for about 3 h with an average count rate of about 1.5×10^3 counts sec^{-1} at $m/z = 102$ ($Cl_2O_2^+$). The pressure of ClOOCl behind the nozzle depended on the amount of solid ClOOCl and the trap temperature, which was controlled with a stability better than ± 0.5 K. The variation of the count rate of ClOOCl was less than ±15%.

Similar to the observation by Pope et al.,[8] the relative concentration between ClOOCl and Cl_2 varied during the evaporation process. There were two major sources of Cl_2: one was from the condensed Cl_2 reagent; the other was from decomposition of ClOOCl. At the beginning stage of a typical experimental run, the Cl_2 was mostly from evaporation of the trapped Cl_2 reagent, resulting in a very high Cl_2 concentration within a short time period (~10 min). We avoided this period for the data acquisition. Under the condition that the ClOOCl count rate was high enough for the cross section measurements, the decomposition of ClOOCl to $Cl_2 + O_2$ in the trapping tube seemed inevitable. The best concentration ratio of ClOOCl to Cl_2 was about 1.5 in our experiments. During a typical data acquisition, this ratio varied slowly from 0.5 (beginning) to 1.5 (near the end).

Mass scan of the sample was regularly checked to ensure the sample purity. Higher chlorine oxides (e.g., Cl_2O_3) were not observed. It is worth to mention that von Hobe et al.[16] reported an absorption spectrum of ClOOCl in a neon matrix. The authors employed the same synthesis method (Method 1 by Pope et al.[8]) and performed a careful impurity check with infrared absorption and Raman scattering spectroscopy. Their results[16] confirmed that this synthesis method is efficient in producing ClOOCl; the only significant impurity is Cl_2; more importantly, possible isomers of Cl_2O_2, such as $ClClO_2$ and ClOClO, would not be produced.

The output of a Nd:YAG pumped dye laser (Continuum ND-6000, 660 nm, ~30 mJ/pulse, 30 Hz) was frequency-doubled by a nonlinear crystal (Type I DKDP, 30 mm long). The laser wavelength was measured by an optical fiber/diode array spectrometer (Ocean Optics Inc., HR4000CG-UV-NIR, 0.75 nm resolution). The pulse energy of the 330 nm laser beam was about 10 mJ, which could be homogeneously attenuated by a dielectric-coated optics (Laseroptik GmbH, Variable Attenuator). The vertical dimension of the laser beam was focused to about 0.5 mm with a cylindrical lens of 500 mm focal length; a pair of cylindrical concave mirrors (Lambda Research Optics, HHR-330 nm coating, 500 mm radial curvature) was used to refocus the laser beam onto the molecular beam. A total of 8 passes of the laser beam were aligned to overlap with the molecular beam. The height of the molecular beam was about 0.3 mm,

which was slightly smaller than the vertical size of the laser spots. The vertical direction of the laser beam was focused on the molecular beam after each pass; in the horizontal direction, the laser beam (3 mm wide) was only collimated and formed a "double-W" pattern, WW. With a burn paper and a slit, we estimated the overall effective laser spot dimensions to be 0.5 mm (vertical) × 21 mm (horizontal). Then, the effective laser fluence was on the order of 1×10^{18} photon cm^{-2}.

The chopper-wheel slit of the molecular beam opened at a repetition rate of 90 Hz, such that the 30 Hz laser beam interacted with one molecular beam pulse for every three pulses. The exit laser beam was monitored by a thermopile power meter (Gentec-EO, UP19K-30H-VM, linearity better than 2.5%).

Results

Under the condition that the number of photons greatly exceeds the number of molecules, an alternative form of Beer's law can be written as

$$\ln \frac{N_0}{N} = I\sigma\phi \tag{1}$$

Where N_0 and N are the number of the molecules before and after the laser irradiation, respectively; I is the laser fluence in number of photons per unit area; σ is the absorption cross section; and ϕ is the dissociation quantum yield. By comparing the photodepletion signal of ClOOCl with that of a reference molecule, it only requires the ratio of the laser fluences to obtain the cross section ratio, as in eq 2.

$$\frac{[\sigma\phi]_{\mathrm{ClOOCl}}}{[\sigma\phi]_{\mathrm{ref}}} = \frac{I_{\mathrm{ref}}}{I_{\mathrm{ClOOCl}}} \frac{\ln(^{N_0}/_{N})_{\mathrm{ClOOCl}}}{\ln(^{N_0}/_{N})_{\mathrm{ref}}} \tag{2}$$

In this work, we chose Cl_2 as the reference molecule. It is known that the involved electronic states of Cl_2 after UV excitations are either repulsive or excited above their thresholds. As a result, lifetimes of the photoexcited Cl_2 are very short (sub-picosecond), leading to 100% dissociation. A similar argument can be applied to ClOOCl, because ab initio calculations[22−24] and molecular beam experiment[25] indicate fast dissociation after UV excitations. The molecular beam results[25] indicate that R1a is the major product channel while R1b is minor; the relative branching ratio of R1a:R1b is (0.9 ± 0.1):(0.1 ± 0.1).

Figure 1 shows the molecular beam signals of ClOOCl and Cl_2 before and after the laser irradiation. Although depletion signals could be observed with a single-pass laser beam, the multipass of the laser beam increased the photolysis volume and resulted in a wider depletion signal in the arrival time. Such a wider signal helped the signal averaging and improved the effective signal-to-noise ratio. In addition, spreading of the depletion signal caused by the finite sizes of the chopper slit and the detector volume became relatively small if a large photolysis volume was used. In Figure 1, the depletion signal of Cl_2 is about 30%, which is consistent with the estimated laser fluence of 1×10^{18} photon cm^{-2}.

The absolute cross sections of ClOOCl can be obtained by analyzing[17] the data with eq 2. Great care was taken to ensure that the ClOOCl and Cl_2 experiments were performed under (nearly) identical conditions. In particular, the identical chopper-to-laser delay time selected the same velocity component of the ClOOCl and Cl_2 beams, resulting in the same depletion time profile, which simplified the analysis. In addition, we dosed a small amount of Cl_2 in the ClOOCl sample, so we could measure the depletion signals of these two molecules almost simultaneously (the detected m/z was switched every 5−10 min). On the basis that Cl_2 does not absorb light at 248 nm, our previous result[20] concluded that ClOOCl would not produce any daughter-ion signal at $m/z = 70$. In this way, the effect of laser instability could be averaged out. The results of the cross section measurements are summarized in Table 1.

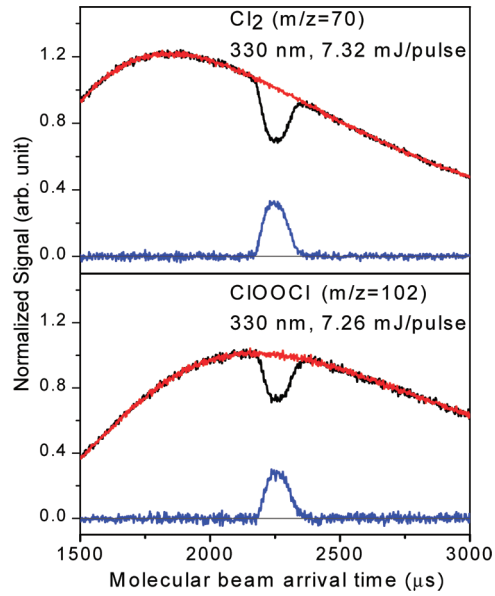

Figure 1. Number density profiles of the molecular beams showing the photodepletion signals at $T = 200$ K. Red and black lines are the molecular beam signals before and after the laser irradiation; blue line is the difference (N_0 − N). The laser delay time and spot size were the same for ClOOCl and Cl_2.

TABLE 1: Summary of the Measured Photodissociation Cross Sections of ClOOCl at 330 nm

	cross section ratio $([\sigma\phi]_{ClOOCl})/([\sigma\phi]_{ref})$				
temperature	mean value	standard deviation[a]	error bar[a]	σ_{ref} (10^{-20} cm^2)[b]	$[\sigma\phi]_{ClOOCl}$ (10^{-20} cm^2)
200 K	0.86	2.7%	±4.8%	26.83	**23.1**
250 K	0.94	3.0%	±5.0%	26.25	**24.7**

[a] Relative to the mean values. The error bars are 1σ (1 standard deviation) and include possible systematic errors (see text). [b] The reference molecule is Cl_2 at the same temperature as the ClOOCl. The absorption cross sections of Cl_2 are taken from the JPL 2006 values.[9] The dissociation yield of Cl_2 is taken as unity.

Possible Error Sources. Our method does not require the knowledge of the absolute concentrations. We have tested the cross section measurements at quite different ClOOCl and Cl_2 beam intensities; no differences in the cross section ratio could be found. The accuracy of our measurements is mainly limited by two factors: the stability of the photolysis laser beam and the accuracy of the reference cross section. The cross sections of Cl_2 have been determined to a very high degree of certainty[9] such that this potential error term can be ignored. Regarding the laser stability, we have repeated the experiment consecutively for a large number of ClOOCl/reference pairs. The average effect of the laser stability would show up in the standard deviations of the cross section ratios, which are about 3% or less (see Table 1).

It is important to mention that only the average value of the laser power and the average molecular depletion signal N/N_0

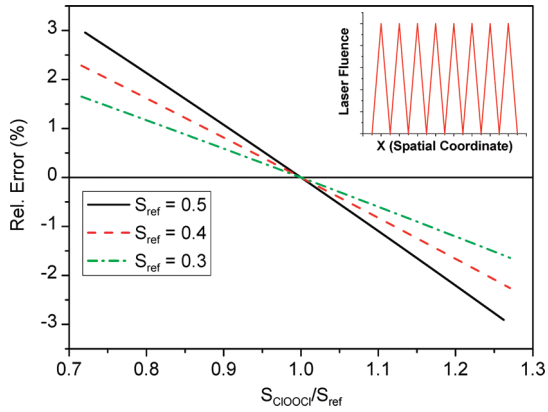

Figure 2. Simulation of the errors due to the nonuniform laser spot in the worst case possible. Vertical axis: percentage error of the determined cross section; horizontal axis: signal ratio of S_{ClOOCl}/S_{ref}. Inset: the laser spatial distribution used in the simulation.

could be recorded. That is, we can only approximate $\langle \ln(N_0/N) \rangle$ by $\ln(\langle N_0/N \rangle)$, such that eq 2a was actually used in the data analysis.

$$\frac{[\sigma\phi]_{ClOOCl}}{[\sigma\phi]_{ref}} \cong \frac{\langle I_{ref} \rangle}{\langle I_{ClOOCl} \rangle} \frac{\ln(\langle {}^{N_0}/_{N} \rangle)_{ClOOCl}}{\ln(\langle {}^{N_0}/_{N} \rangle)_{ref}} = \frac{\langle I_{ref} \rangle}{\langle I_{ClOOCl} \rangle} \frac{S_{ClOOCl}}{S_{ref}} \tag{2a}$$

Where the bracket $\langle\rangle$ means taking the average value, and we define the depletion signal $S = \ln(\langle N_0/N \rangle)$ for convenience. For a stable and homogeneous laser spot, the laser fluence I is a single value, and there will be no error in the approximation of eq 2a. But in the practical situation, there is a considerable variation in the laser fluence I, especially due to the nonuniform spatial distribution of the laser spot. In order to estimate the corresponding error, we performed a simulation in which a triangular function was assumed to represent the spatial distribution of each laser pass. (This would be the worst case. Practically there was some overlap between the laser beams, such that the valleys were not as deep.) The results are plotted in Figure 2.

In Figure 2 we can see that the error is 0 when the signal ratio is 1. This simply represents a condition that if the average values are the same, the individual values will also be the same for a given distribution. When the signal ratio is larger than 1, the nonlinearity of the logarithm function in eq 2a leads to underestimation of the cross section ratio (negative error), and vice versa. This can be viewed as a local saturation effect that the most intense part of the laser spot does not contribute linearly to the depletion signal S, because the averaging operation is inside the logarithm function. Fortunately, the error is significantly reduced when S is small, simply because the logarithm function $\ln(x)$ can be approximated by a linear function [$\ln(x) \cong x - 1$] when x is close to 1. In our experiments, the depletion signals S were controlled to be less than 0.4 and the signal ratios S/S_{ref} were in the range of 0.85−1.1. Therefore, the error arising from the nonuniform laser spot can be estimated to be less than 2%.

Experimentally we could check the ClOOCl and Cl_2 depletion signals at various laser fluences. As shown in Figure 3, there the depletion signal S increases linearly with the laser fluence I, indicating that the saturation effects are insignificant in our experiments.

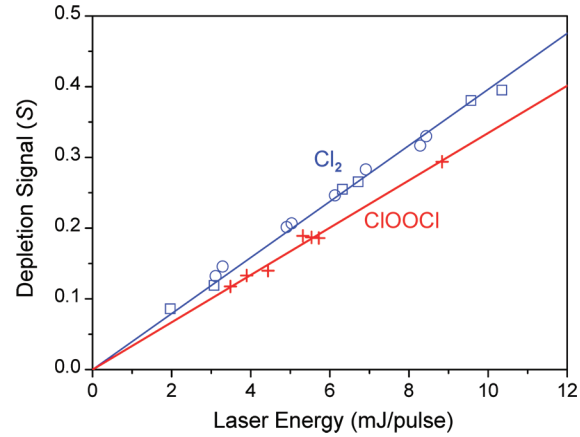

Figure 3. Depletion signal S of Cl_2 and ClOOCl at various laser fluence I. The laser fluence was proportional to the pulse energy and was homogenously attenuated by a dielectric-coated optics. The circle and square symbols indicate the experimental data of Cl_2 at two different days.

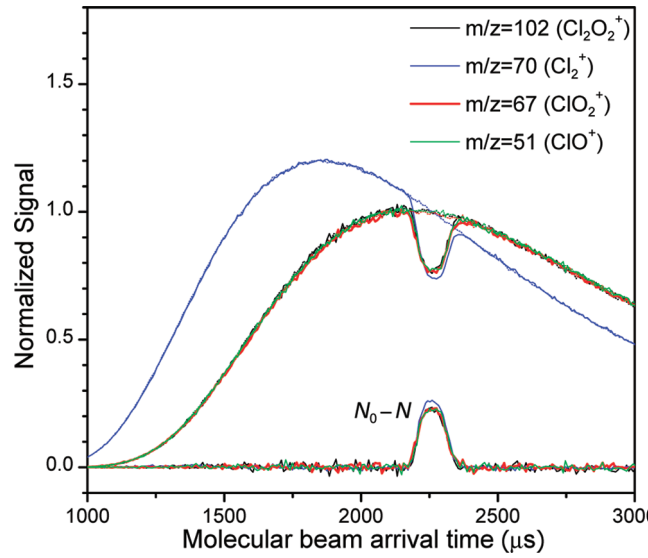

Figure 4. Normalized molecular beam signals (number density) at different ionic masses recorded under very similar experimental conditions. The data at T = 200 K are shown; the data at 250 K are similar. Dotted lines: laser off; solid lines: laser on, and the differences between signals of laser on and laser off.

Figure 4 shows the molecular beam signals at a few representative ionic masses (m/z = 51, 67, 70, and 102). In an effusive molecular beam, the velocity of a molecule is proportional to the square root of the temperature−mass ratio.

$$v \propto \sqrt{T/m_n} \tag{3}$$

Where m_n is the mass of the neutral molecule. Upon electron impact ionization, fragmentation of the ion may occur and this leads to various daughter masses. In Figure 4, we can see the arrival-time distributions at m/z = 102, 67, and 51 are nearly identical. This perfect match provides strong evidence that all these ions are originated from the same neutral species ClOOCl. It is obvious that the m/z = 70 signal arises from a different species—Cl_2. To be more quantitative, we performed analyses with eq 3 on the arrival-time distributions in Figure 4. If there was a small amount of ClO_2 contributing to the signals at m/z = 67 or 51, the relative contribution would be 2% or less,

otherwise the simulation would not fit the measured arrival time distributions. Similarly, the ClO contribution to the signal at $m/z = 51$ should be less than 1%.

Another important information in Figure 4 are the intensities of the laser-depleted signals, $N_0 - N$. The laser fluences used for the four masses were nearly identical. The laser-off signals were normalized to the same height at the time of the maximum depletion. We can see in Figure 4 that the cross section of Cl_2 is the largest, and the cross sections observed at other masses are nearly identical. Analysis with eq 2a shows that the differences among the cross sections obtained from the data at $m/z = 51$, 67, and 102 are less than 2%. This observation indicates that the quadrupole mass filter (in the detector) operated at different m/z did not affect the cross section determination at all. It is known that the size of the effective entrance aperture of a quadrupole mass filter is a function of the mass resolution and m/z setting. If the overlap between the laser-irradiated molecular beam and the entrance aperture of the quadrupole mass filter varies with m/z, some systematic error might be introduced because the laser beam was not very uniform, and we usually detected ClOOCl at $m/z = 102$ and the reference molecules (Cl_2, in this work; Cl_2, Cl_2O or O_3 in previous works[17,20]) at smaller masses. The fact that detection of the smaller fragment ions at $m/z = 67$ and 51 yields essentially the same results as the detection of the parent ClOOCl ion at $m/z = 102$ shows that any errors resulting from m/z dependent overlap are insignificant in our experiment.

The nonlinearity of the laser power meter is less than 2.5%, according to the manufacturer, which might also contribute to the systematic error. From the above error analyses, we think the major contributions of systematic errors are from (i) nonuniform laser spot (2% or less); (ii) different detected masses for ClOOCl and Cl_2 (2% or less); and (iii) laser power measurements (2.5% or less). If we take an incoherent sum of these errors, the maximum overall systematic error can be estimated as $(0.02^2 + 0.02^2 + 0.025^2)^{1/2} = 0.038 \cong 4\%$. Together with random errors that would show up in the standard deviation of the cross section ratio, we estimate the final percentage error by the expression:

$$\pm\sqrt{(\beta/\alpha)^2 + 0.04^2} \times 100\% \qquad (4)$$

where α is the cross section ratio and β is the standard deviation of α (See Table 1).

Temperature Dependence. The precision of our method allows us to observe the temperature dependence of the ClOOCl photolysis cross section. From Table 1, we can see that the cross section of ClOOCl at 330 nm is larger at the higher temperature; it increases by 7% from 200 to 250 K. Although comparable to the magnitude of the error bars, this temperature effect was consistently observed in all experimental runs. Since the temperature effect is a relative quantity, the measurement error bar is less than that for the absolute cross section. The temperature effect at 330 nm is smaller than that at 351 nm (+12%, 200−250 K),[17] but was significantly larger than that at 308 nm (+4%, 200−250K).[17] This observation suggests that the temperature effect of the cross section may become larger at longer wavelengths.

Von Hobe et al.[16] measured the absorption spectrum of ClOOCl in a neon matrix at a temperature of 6 K. The authors carefully checked the sample purity by infrared and Raman spectroscopy and showed that the impurity level was insignificant after their purification process. However, they only measured a relative absorption spectrum, not an absolute one. Therefore we should only compare the relative values of the cross sections. The ratio of the measured cross sections σ(330 nm)/σ(248 nm) by von Hobe et al. is about 12.6/610 = 0.021, which is roughly 19% smaller than our corresponding value 23.1/885 = 0.026 [this work and ref 20 at $T = 200$K]. Because the temperature effect at 248 nm[20] is much smaller and of opposite sign, it is expected to see a smaller cross section ratio α(330 nm)/α(248 nm) at lower temperatures.

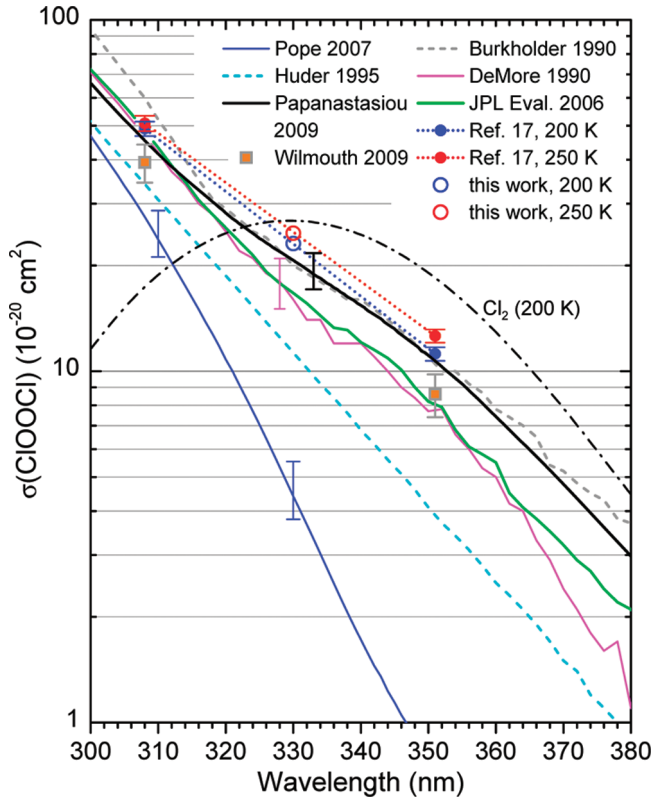

Figure 5. Comparison of a few measurements[8−12,18,19] and our molecular beam results (ref 17 and this work) of the ClOOCl cross sections in a wavelength region of 300−380 nm, which is the most relevant region for its atmospheric photolysis rates. The reported error bars are shown selectively to avoid crowding the figure. The absorption spectrum of Cl_2 at 200 K[9] is shown as a dash-dotted line.

The temperature in the stratosphere is of course not a constant. Therefore, the temperature-dependent cross sections of ClOOCl would improve the accuracy in estimating the temperature-dependent photolysis rates of ClOOCl in the stratosphere.

Discussions

A comparison of a few measurements[8−12,18,19] of the ClOOCl cross sections with our results is given in Figure 5. Burkholder et al.[10] averaged their data over a temperature range of 205−250 K and reported the cross section at 330 nm to be 20×10^{-20} cm^2. New measurement by Papanastasiou, Burkholder, and co-workers[19] gives a similar cross section value of $20.7^{+2.8}_{-1.8} \times 10^{-20}$ cm^2 at 330 nm and 200−228 K. The results by Papanastasiou et al.[19] were based on subtraction of spectral curves of which the accuracy would rely on the linearity of the spectrometer. Although these two results[10,19] are roughly consistent with this work at 330 nm after considering the ranges of the error bars, their reported cross sections at 248 and 266 nm are somewhat lower than our corresponding values.[20] The cross sections at 330 nm reported by other works[8,9,11,12] are significantly smaller than the cross section values given in Table 1. We think the discrepancy in these spectroscopic measure-

ments[8−12,19] is due to the small ClOOCl absorbance and relatively large impurity absorbance at this and longer wavelengths. On the other hand, the directness and simplicity of our method should provide more reliable results.

Wilmouth et al.[18] performed a new type of measurements in which Cl_2 and the Cl-atom products from photolysis of ClOOCl and Cl_2 were measured simultaneously. To obtain absolute cross sections at 308 and 352 nm, the authors employed two methods for the calibration. In their Method 1, the observed signal from ClOOCl at 308 or 352 nm was referenced to the observed signal and the JPL 2006 cross section[9] of ClOOCl at 248 nm. If they referenced their measurements to our cross section value at 248 nm (873×10^{-20} cm^2 at 260 K),[20] the resulting cross sections would become

$$873 \times 10^{-20}\text{cm}^2/17.0 = 51.4 \times 10^{-20}\text{cm}^2 \text{ at } 308 \text{ nm}$$

$$873 \times 10^{-20}\text{cm}^2/72.2 = 12.1 \times 10^{-20}\text{cm}^2 \text{ at } 352 \text{ nm}$$

These values are in fact quite close to our previous results.[17] Their Method 2 relies on the conservation of chlorine between Cl_2 and ClOOCl in their microwave discharge−flow tube reactor. However, the cross sections obtained by their Method 2 are 40.2×10^{-20} cm^2 at 308 nm and 8.54×10^{-20} cm^2 at 352 nm,[18] which are significantly smaller than our values.[17] One point should be considered for this comparison: the values we measured are $\sigma\phi_{\text{diss}}$, whereas the values of Wilmouth et al. are $\sigma\phi_{\text{Cl}}$. If we take $\phi_{\text{Cl}}/\phi_{\text{diss}} = 0.9$,[25] that is, the yield of R1a is 90% instead of 100%, then the $\sigma\phi_{\text{diss}}$ values deduced from the results by Method 2 of Wilmouth et al. would become

$$(40.2 \pm 3.2) \times 10^{-20}\text{cm}^2/0.9 = (44.7 \pm 3.6) \times 10^{-20}\text{cm}^2 \text{ at } 308 \text{ nm}$$

and

$$(8.54 \pm 0.94) \times 10^{-20}\text{cm}^2/0.9 = (9.49 \pm 1.04) \times 10^{-20}\text{cm}^2 \text{ at } 352 \text{ nm}$$

and the discrepancy would become smaller.

Considering the molecular beam results of the ClOOCl cross sections at 308, 330, and 351 nm (ref 17 and this work), the data points at the same temperature lie on a straight line on the log−linear plot as shown in Figure 5. Because spectroscopic studies[9−16,19] of ClOOCl all indicate a broad and featureless spectrum, a linear line on the log−linear plot may be a good approximation for the ClOOCl cross sections between 308 and 351 nm.

Model calculations[5,6] and field measurements[6] of ClO, ClOOCl, and O_3 loss rates are getting more consistent if the ClOOCl cross sections by Burkholder et al.[10] are used. The cross section of the Burkholder et al. curve is slightly above our results at 308 nm, but is slightly lower than our values at 330 and 351 nm (see Figure 5). Therefore, our data would suggest a little bit higher atmospheric photolysis rate of ClOOCl than using the values of Burkholder et al., considering that the solar flux is higher at longer wavelengths.

Concluding Remarks

The experimental method in this series of works was designed to circumvent the difficulties of impurity subtraction that might have caused some errors in conventional measurements of the ClOOCl absorption cross sections. A difficulty of this approach is the need of a high intensity laser. Our previous works[17,20] were limited in the excimer-laser and YAG-laser wavelengths. This work utilized a multipass technique to enhance the effective laser fluence and photolysis volume, such that a tunable laser source (dye laser) could produce enough signals for the cross section determination.

The photodissociation cross section of ClOOCl at 330 nm was determined at 200 and 250 K; a significant temperature effect was observed. The combination of the improved spectral curves[16,19] and the more accurate single-wavelength results at 308, 330, and 351 nm (ref 17 and this work) would not only resolve the debate on the validity of current photochemical models for the ozone depletion, but also narrow down the error bars in estimating the atmospheric photolysis rates of ClOOCl.

Some uncertainty of the Cl-atom production rate from ClOOCl lies on the uncertainty of the branching ratio between R1a and R1b. We are setting up a new experiment to measure the products of the ClOOCl photolysis and to determine a more precise branching ratio, which would improve the estimation of the Cl-atom production rate in the atmosphere.

Acknowledgment. This work is supported by Academia Sinica and National Science Council (NSC 98-2113-M-001-027-MY2), Taiwan. The authors thank Professor Yuan T. Lee for insightful discussions.

References and Notes

(1) World Meteorological Organization (WMO). *Scientific Assessment of Ozone Depletion: 2006*; WMO, Global ozone research and monitoring project, Report no. 50: Geneva, Switzerland, 2007; http://ozone.unep.org/Assessment_Panels/SAP/Scientific_Assessment_2006. Accessed February 2007.

(2) Cox, R. A.; Hayman, G. D. *Nature* **1988**, *332*, 796.

(3) von Hobe, M. *Science* **2007**, *318*, 1878.

(4) Sander, S. P.; Friedl, R. R.; Yung, Y. L. *Science* **1989**, *245*, 1095.

(5) von Hobe, M.; Salawitch, R. J.; Canty, T.; Keller-Rudek, H.; Moortgat, G. K.; Grooss, J.-U.; Muller, R.; Stroh, F. *Atmos. Chem. Phys.* **2007**, *7*, 3055.

(6) Stimpfle, R. M.; Wilmouth, D. M.; Salawitch, R. J.; Anderson, J. G. *J. Geophys. Res.* **2004**, *109*, D03301.

(7) Molina, L. T.; Molina, M. J. *J. Phys. Chem.* **1987**, *91*, 433.

(8) Pope, F. D.; Hansen, J. C.; Bayes, K. D.; Friedl, R. R.; Sander, S. P. *J. Phys. Chem. A* **2007**, *111*, 4322.

(9) Sander, S. P.; Ravishankara, A. R.; Golden, D. M.; Kolb, C. E.; Kurylo, M. J.; Molina, M. J.; Moortgat, G. K.; Finlayson-Pitts, B. J.; Wine, P. H.; Huie, R. E.; Orkin, V. L. *Chemical Kinetics and Photochemical Data for Use in Atmospheric Studies. Evaluation Number 15, JPL Publication 06−2*; Jet Propulsion Laboratory: Pasadena, CA, 2006.

(10) Burkholder, J. B.; Orlando, J. J.; Howard, C. J. *J. Phys. Chem.* **1990**, *94*, 687.

(11) DeMore, W. B.; Tschuikow-Roux, E. *J. Phys. Chem.* **1990**, *94*, 5856.

(12) Huder, K. J.; DeMore, W. B. *J. Phys. Chem.* **1995**, *99*, 3905.

(13) Permien, T.; Vogt, R.; Schindler, R. N. In *Mechanics of Gas Phase and Liquid Phase Chemical Transformations. Air Pollution Report, No. 17*; Environmental Research Program of the CEC, EUr 12035 EN; Cox, R. A. Ed.; Brussels, Belgium, 1988; pp 149−153.

(14) McKeachie, J. R.; Appel, M. F.; Kirchner, U.; Schindler, R. N.; Benter, T. *J. Phys. Chem. B* **2004**, *108*, 16786.

(15) Stratospheric Processes and Their Role in Climate (SPARC), The Role of Halogen Chemistry in Polar Stratospheric Ozone Depletion: Report from the June 2008 Cambridge, UK Workshop for an Initiative under the Stratospheric Processes and Their Role in Climate (SPARC) Project of the World Climate Research Programme; 2009. Available at http://www.atmosp.physics.utoronto.ca/SPARC/HalogenChem_Final_20090213.pdf.

(16) von Hobe, M.; Stroh, F.; Beckers, H.; Benter, T.; Willner, H. *Phys. Chem. Chem. Phys.* **2009**, *11*, 1571.

(17) Chen, H. Y.; Lien, C. Y.; Lin, W. Y.; Lee, Y. T.; Lin, J. J. *Science* **2009**, *324*, 781.

(18) Wilmouth, D. M.; Hanisco, T. F.; Stimpfle, R. M.; Anderson, J. G. *J. Phys. Chem. A* **2009**, DOI: 10.1021/jp9053204.

(19) Papanastasiou, D. K.; Papadimitriou, V. C.; Fahey, D. W.; Burkholder, J. B. *J. Phys. Chem. A* **2009**, *113*, 13711.
(20) Lien, C.-Y.; Lin, W.-Y.; Chen, H.-Y.; Huang, W.-T.; Jin, B.; Chen, I.-C.; Lin, J. J. *J. Chem. Phys.* **2009**, *131*, 174301.
(21) Lin, J. J.; Hwang, D. W.; Harich, S.; Lee, Y. T.; Yang, X. *Rev. Sci. Instrum.* **1998**, *69*, 1642.
(22) Kaledin, A. L.; Morokuma, K. *J. Chem. Phys.* **2000**, *113*, 5750.
(23) Toniolo, A.; Granucci, G.; Inglese, S.; Persico, M. *Phys. Chem. Chem. Phys.* **2001**, *3*, 4266.
(24) Peterson, K. A.; Francisco, J. S. *J. Chem. Phys.* **2004**, *121*, 2611.
(25) Moore, T. A.; Okumura, M.; Seale, J. W.; Minton, T. K. *J. Phys. Chem. A* **1999**, *103*, 1691.

JP909374K